

Spectral and optical properties in the antiphase stripe phase of the cuprate superconductors

Hong-Min Jiang,¹ Cui-Ping Chen,¹ and Jian-Xin Li¹

¹*National Laboratory of Solid State of Microstructure and Department of Physics, Nanjing University, Nanjing 210093, China*
(Dated: November 2, 2018)

We investigate the superconducting order parameter, the spectral and optical properties in a stripe model with spin (charge) domain-derived scattering potential V_s (V_c). We show that the charge domain-derived scattering is less effective than the spin scattering on the suppression of superconductivity. For $V_s \gg V_c$, the spectral weight concentrates on the $(\pi, 0)$ antinodal region, and a finite energy peak appears in the optical conductivity with the disappearance of the Drude peak. But for $V_s \approx V_c$, the spectral weight concentrates on the $(\pi/2, \pi/2)$ nodal region, and a residual Drude peak exists in the optical conductivity without the finite energy peak. These results consistently account for the divergent observations in the ARPES and optical conductivity experiments in several high- T_c cuprates, and suggest that the "insulating" and "metallic" properties are intrinsic to the stripe state, depending on the relative strength of the spin and charge domain-derived scattering potentials.

PACS numbers: 74.20.Mn, 74.25.Ha, 74.25.Jb, 74.72.Bk

I. INTRODUCTION

The nature of spin and/or charge inhomogeneities, especially in the form of stripes, in some cuprates and their involvement to high-temperature superconductivity are currently debate issues.¹ The stripe state is characterized by the self-organization of the charges and spins in the CuO_2 planes in a peculiar manner, where the doped holes are arranged in one-dimensional (1D) lines and form the so-called "charge stripe" separating the antiferromagnetic domains. The stripe-ordered state minimizes the energy of the hole-doped antiferromagnetic system, thus leading to an inhomogeneous state of matter. Static one-dimensional charge and spin stripe order have been observed experimentally in a few special cuprate compounds, specifically in $\text{La}_{1.6-x}\text{Nd}_{0.4}\text{Sr}_x\text{CuO}_4$ ^{2,3} and $\text{La}_{2-x}\text{Ba}_x\text{CuO}_4$ with $x = 1/8$.^{4,5} Similar signatures identified in $\text{La}_{2-x}\text{Sr}_x\text{CuO}_4$ (LSCO)^{6,7,8,9} and other high temperature superconductors^{10,11,12} point to the possible existence of stripes, albeit of a dynamical or fluctuating nature.

A pivotal issue about this new electronic state of matter concerns whether it is compatible with superconductivity, and possibly even essential for the high transition temperatures, or it competes with the pairing correlations. A prerequisite for addressing these issues is to understand the electronic structures of various stripe states in different cuprates, and to answer the question whether the stripe phase is intrinsically "metallic" or "insulating", given its spin- and charge-ordered nature. Angle-resolved photoemission spectroscopy (ARPES) study by Zhou *et al.* in $(\text{La}_{1.28}\text{Nd}_{0.6}\text{Sr}_{0.12})\text{CuO}_4$ with static stripes have found the depletion of the low-energy excitation near the $(\pi/2, \pi/2)$ nodal region.³ In another compound $\text{La}_{1.875}\text{Ba}_{0.125}\text{CuO}_4$, a system where the superconductivity is heavily suppressed due to the development of the static spin and charge orders, Valla *et al.* have detected

the high spectral intensity of the low-energy excitation in the vicinity of the $(\pi/2, \pi/2)$ nodal region [while antinodal low-energy quasiparticle near $(0, \pi)$ are gapped].¹³ The compound $(\text{La}_{1.4-x}\text{Nd}_{0.6}\text{Sr}_x)\text{CuO}_4$ ($x = 0.10$ and 0.15) with static one-dimensional stripe, seems to be an in-between system, in where the existence of spectral weight around the nodal region, though weak, has been identified.¹⁴

Meanwhile, optical conductivity measurements on the systems with a stripe phase also display the divergent results. In $\text{La}_{1.275}\text{Nd}_{0.6}\text{Sr}_{0.125}\text{CuO}_4$ ¹⁵ and $\text{La}_{1.875}\text{Ba}_{0.125-x}\text{Sr}_x\text{CuO}_4$,¹⁶ a finite frequency absorption peak with almost disappearance of the Drude mode in the low-frequency conductivity in several experiments has been interpreted as collective excitations of charge stripes or as charge localization from the disorder created by Nd or Ba substitutions. These observations may support the suggestion that such stripe-ordered state should be "insulating" in nature.¹⁷ On the other hand, optical experiment on $\text{La}_{1.875}\text{Ba}_{0.125}\text{CuO}_4$ ¹⁸ has observed a residual Drude peak with a loss of the low-energy spectral weight below the temperature corresponding to the onset of charge stripe order, which indicates that stripes are compatible with the so-called nodal-metal state.^{18,19,20,21,22,23}

Although, there have been some theoretical studies on the spectral and optical properties in the stripe phase in the past years,^{24,25,26,27} the contradictory observations in recent experiments as mentioned above have yet not been explained consistently in theoretical frame by adopting a realistic stripe model. In this paper, by using a stripe model in which the experimentally observed spin and charge structures at $1/8$ doping are well reflected, we show that the spin domain-derived scattering will depress the zero-energy spectral weight around the nodal regions, while the charge domain-derived scattering will suppress mostly those around the antinodal regions and the hot spots. Compared to the ARPES data, this sug-

gests that the different spectral weight distribution may result from the different relative strength of the spin and charge domain-derived scattering potentials inherently existing in these compounds. Meanwhile, a finite frequency peak in the optical conductivity appears with the disappearance of the Drude peak in the case of the dominant spin domain-derived scattering. While, when the charge domain-derived scattering is comparable to the spin one, a residual Drude peak exists with the disappearance of the finite energy peak. This suggests that both the "insulating" and "metallic" properties are intrinsic to the stripe state without introducing another distinct metallic phase.

The rest of this paper is organized as follows. In Sec. II, we introduce the model Hamiltonian and carry out the analytical calculations. In Sec. III, we present the numerical calculations and discuss the results. In Sec. IV, we present the conclusion.

II. THEORY AND METHOD

As the above discussed compounds have a doping density at or near 1/8, we will in this paper consider the 1/8 doping antiphase vertical stripe state. A schematic illustration of its charge and spin pattern is presented in Fig. 1. The charge stripes, with a unit cell of 8 lattice sites

(Note for 1/8 doping, there is one hole for every two sites along the length of a charge stripe), act as antiphase domain walls for the magnetic order, so that the magnetic unit cell is twice as long as that for charge order. Due to the periodical modulation of the stripe order, the electrons moving in the state will be scattered by the modulation potentials. After Fourier transformation, the potential V_n can be written as the scattering term between the state k and those at $k \pm nQ$ with $Q = (3\pi/4, \pi)$. Following Ref. 28, we expect that the terms V_1 and V_2 will be the dominant spin and charge domain-derived scattering term, and will be relabeled as V_s and V_c in the following, respectively. The weaker higher harmonic terms will be neglected here. In the coexistence with the superconducting (SC) order, the model Hamiltonian can be written as a 16×16 matrix for k in the reduced Brillouin zone,

$$\hat{H} = \sum_k {}' \hat{C}^\dagger(k) \begin{pmatrix} \hat{H}_k & \hat{\Delta}_k \\ \hat{\Delta}_k & -\hat{H}_k \end{pmatrix} \hat{C}(k), \quad (1)$$

where, the prime denotes the summation over the reduced Brillouin zone. \hat{C}_k is a column vector with its elements $C_i(k) = C_{k+(i-1)Q, \uparrow}$ for $i = 1, 2, \dots, 8$, and $C_{-k-(i-9)Q, \downarrow}^\dagger$ for $i = 9, 10, \dots, 16$. Both \hat{H}_k and $\hat{\Delta}_k$ are 8×8 matrix with

$$\hat{H}_k = \begin{pmatrix} \varepsilon_k & V_s & V_c & 0 & 0 & 0 & V_c & V_s \\ V_s & \varepsilon_{k+Q} & V_s & V_c & 0 & 0 & 0 & V_c \\ V_c & V_s & \varepsilon_{k+2Q} & V_s & V_c & 0 & 0 & 0 \\ 0 & V_c & V_s & \varepsilon_{k+3Q} & V_s & V_c & 0 & 0 \\ 0 & 0 & V_c & V_s & \varepsilon_{k+4Q} & V_s & V_c & 0 \\ 0 & 0 & 0 & V_c & V_s & \varepsilon_{k+5Q} & V_s & V_c \\ V_c & 0 & 0 & 0 & V_c & V_s & \varepsilon_{k+6Q} & V_s \\ V_s & V_c & 0 & 0 & 0 & V_c & V_s & \varepsilon_{k+7Q} \end{pmatrix}, \quad (2)$$

and

$$\hat{\Delta}_k = \begin{pmatrix} \Delta_k & 0 & 0 & 0 & 0 & 0 & 0 & 0 \\ 0 & \Delta_{k+Q} & 0 & 0 & 0 & 0 & 0 & 0 \\ 0 & 0 & \Delta_{k+2Q} & 0 & 0 & 0 & 0 & 0 \\ 0 & 0 & 0 & \Delta_{k+3Q} & 0 & 0 & 0 & 0 \\ 0 & 0 & 0 & 0 & \Delta_{k+4Q} & 0 & 0 & 0 \\ 0 & 0 & 0 & 0 & 0 & \Delta_{k+5Q} & 0 & 0 \\ 0 & 0 & 0 & 0 & 0 & 0 & \Delta_{k+6Q} & 0 \\ 0 & 0 & 0 & 0 & 0 & 0 & 0 & \Delta_{k+7Q} \end{pmatrix}. \quad (3)$$

As for the tight-binding energy band, we will choose the following form,^{29,30}

$$\begin{aligned} \varepsilon_k = & -2(\delta t + J' \chi_0)(\cos k_x + \cos k_y) \\ & -4\delta t' \cos k_x \cos k_y - \mu. \end{aligned} \quad (4)$$

where, δ is the doping density, and a d -wave SC order parameter $\Delta_k = 2J \Delta_0(\cos k_x - \cos k_y)$ is assumed. Gener-

ally, the charge modulation will induce the modulation of the SC order leading to the finite momentum pairs. However, in the present study, one of our aim is to examine the effect of the spin (charge) domain-derived scattering on the SC order. In this regard, the average value of the SC order parameter is relevant and the modulation of the SC order will be ignored. We have checked the effect of this modulation and found no qualitative change in the results presented in Fig. 2. In the following, $J = 100\text{meV}$ is taken as the energy unit, $t = 2J$, $t' = -0.45t$, $J' = \frac{3}{8}J$. This dispersion can be derived from the slave-boson mean-field calculation of the $t - t' - J$ model^{29,30}, and in this way the parameters Δ_0 , χ_0 and μ are determined self-consistently. Here we

take it as a phenomenological form. In a self-consistent calculation, the Hamiltonian is first diagonalized by a unitary matrix $\hat{U}(k)$ with a set of trial values of Δ_0 , χ_0 and μ for given potentials V_s and V_c . Then Δ_0 , χ_0 and μ are self-consistently calculated by using the relations: $\pm\Delta_0 = \langle c_{i\uparrow}c_{i+\tau\downarrow} - c_{i\downarrow}c_{i+\tau\uparrow} \rangle$ (To get the d -wave pairing, the sign before Δ_0 takes $+$ for $\tau = \pm\hat{x}$ and $-$ for $\tau = \pm\hat{y}$, where \hat{x} and \hat{y} denote the unit vectors along x and y directions, respectively.), $\chi_0 = \sum_{\sigma} \langle c_{i\sigma}^{\dagger}c_{j\sigma} \rangle$, and $n = \sum_{\sigma} \langle c_{i\sigma}^{\dagger}c_{i\sigma} \rangle$, respectively. Reformularization of the expressions of Δ_0 , χ_0 and μ in terms of eigenfunctions and eigenvalues of the Hamiltonian, one obtains the self-consistency relations

$$\begin{aligned}\Delta_0 &= -\frac{1}{N} \sum_k (\cos k_x - \cos k_y) \sum_{m=1}^{16} U_{1m}(k) U_{m9}^{\dagger}(k) f[E_m(k)] \\ \chi_0 &= \frac{1}{N} \sum_k (\cos k_x + \cos k_y) \sum_{m=1}^{16} U_{1m}(k) U_{m1}^{\dagger}(k) f[E_m(k)] \\ n &= \frac{2}{N} \sum_k \sum_{m=1}^{16} U_{1m}(k) U_{m1}^{\dagger}(k) f[E_m(k)],\end{aligned}\quad (5)$$

where, $E_m(k)$ is the eigenvalue of the Hamiltonian, $U_{mn}(k)$ the elements of the matrix $\hat{U}(k)$, and $f[E_m(k)]$ is the Fermi-Dirac distribution function.

Then, the single particle Green functions $G_{ij}(k, i\omega_n) = -\int_0^{\beta} d\tau \exp^{i\omega_n\tau} \langle T_{\tau} C_i(k, i\tau) C_j^{\dagger}(k, 0) \rangle$ can be expressed as

$$G_{ij}(k, i\omega_n) = \sum_{m=1}^{16} \frac{U_{im}(k) U_{mj}^{\dagger}(k)}{i\omega_n - E_m(k)}, \quad (6)$$

and the spectral functions is

$$A_{ij}(k, \omega) = -\frac{1}{\pi} \text{Im} G_{ij}(k, \omega + i0^+). \quad (7)$$

III. RESULTS AND DISCUSSION

A. Self-consistent calculation of the SC order parameter

We first present in Fig. 2 the self-consistent results of the SC order parameter as a function of V_s and V_c . While the scattering from both spin and charge domain-derived scattering potentials in the stripe state leads to the suppression of the SC order parameter, the charge domains are more compatible with superconductivity than spin domains, as can be seen from Fig. 2(a). This may support the statement that the SC pairing in the stripe state

occurs most strongly within the charge stripes.³¹ On the other hand, an interesting feature is that the SC order parameter will be zero at the spin domain-derived scattering potential $V_{sc} \approx 0.14$ in the absence of the charge domain-derived scattering, however, it will develop a noticeable value after turning on the charge domain-derived scattering potential, as shown in Fig. 2(b). This shows that the charge domain-derived scattering will lead to the emergency of the SC order which is otherwise destroyed by the spin only scattering.

B. Distribution of spectral weight

In Fig. 3, we present the distribution of the low-energy spectral weight in the original Brillouin zone (integrated over an energy window $\Delta\epsilon = 0.1J$ about ϵ_F) in the 1/8 antiphase stripe state for different spin (charge) domain-derived scattering potential V_s (V_c). Let us first look at the limit where only the spin domain-derived scattering is included, i.e., $V_c = 0$ with $V_s = 0.15$, one will find that the spectral weight around the nodal region is suppressed heavily[See Fig. 3(a)]. At another limit where only the charge domain-derived scattering is included ($V_c = 0.17$ with $V_s = 0$), the spectral weight around the nodal region is recovered and those around the hot spot (the cross of the Fermi surface with the line $k_x \pm k_y = \pm\pi$) and near the antinodal region are suppressed[See Fig. 3(b)]. Starting from the limit of $V_c = 0$

and fixing $V_s = 0.15$, the spectral weight will redistribute gradually from the antinodal region to the nodal region with the increase of the charge domain-derived scattering potential V_c , as shown in Figs. 3(c) and (d). When two scattering potentials are comparable, the strongest spectral weight situates around the nodal region, and at the meantime noticeable spectral weights along the whole Fermi surface is presented. Therefore, the divergent features observed in ARPES measurements by Zhou *et al.* in $(\text{La}_{1.28}\text{Nd}_{0.6}\text{Sr}_{0.15})\text{CuO}_4$ ¹⁴ in which the low-energy excitations near the nodal region are depleted, and by Valla *et al.* in $\text{La}_{1.875}\text{Ba}_{0.125}\text{CuO}_4$ ¹³ in which the high spectral intensity of the low-energy excitation in the vicinity of the nodal region is detected are consistently reproduced here by a change of the relative strength between the charge and spin domain-derived scatterings. This consistent accounting enables us to propose that the spin domain-derived scattering dominates over the charge one in the former system while the scattering strengths of them are comparable in the latter system.

In the presence of the spin (charge) domain-derived potential, quasiparticles near the Fermi surface will be scattered from \mathbf{k} to $\mathbf{k} \pm n\mathbf{Q}$ ($n=1$ for the spin domain-derived potential, $n=2$ for the charge one), for the 1/8 antiphase vertical stripe configuration shown as Fig. 1. This gives rise to two scattering channels from the spin domain with potential V_s ,

$$\begin{aligned} \mathbf{k} &\rightarrow \mathbf{k} + Q = \mathbf{k} + (3\pi/4, \pi), \\ \mathbf{k} &\rightarrow \mathbf{k} - Q = \mathbf{k} + (5\pi/4, \pi), \end{aligned} \quad (8)$$

and two scattering channels from the charge domain with potential V_c ,

$$\begin{aligned} \mathbf{k} &\rightarrow \mathbf{k} + 2Q = \mathbf{k} + (3\pi/2, 0), \\ \mathbf{k} &\rightarrow \mathbf{k} - 2Q = \mathbf{k} + (\pi/2, 0). \end{aligned} \quad (9)$$

Strong potential scattering will destruct those parts of the Fermi surface connected by the above mentioned scattering wave vectors. Because the scattering wave vectors Q and $-Q$ are close to the transferred momenta from the node to node scattering, so it will lead to a depletion of the spectral weight near the nodal region as shown in Fig. 3(a). On the other hand, the scattering wave vectors $2Q$ and $-2Q$, which is near the connecting wave vectors between the two approximately parallel segments of the Fermi surface near the antinodal and hot spot region, the scatterings with these wave vectors will suppress the spectral weights around the antinodal and hot spot regions [Fig. 3(b)].

C. In-plane optical conductivity

Now, we turn to the discussion of the in-plane optical properties in the 1/8 antiphase stripe state, and to see how they are influenced by the scattering from the spin and charge domains. We will fix the temperature at $T = 0.05$ in all calculations, in order to avoid

the influence from the temperature induced change in the scattering rate. We consider an electric field applied in the x direction, which is perpendicular to the stripe. From the Kubo formula for the optical conductivity, the real part of the optical conductivity is $\sigma_1(\omega) = -\lim_{q \rightarrow 0} \text{Im}[\Pi(q, \omega)]/\omega$. The imaginary part of the current-current correlation function $\text{Im}[\Pi(q \rightarrow 0, \omega)]$ is given by

$$\begin{aligned} \text{Im}[\Pi(q \rightarrow 0, \omega)] &= \frac{\pi}{N} \sum_k' \sum_{j,l=1}^{16} v^{jj}(k) v^{ll}(k) \\ &\times \int d\omega' [f(\omega + \omega') - f(\omega')] \\ &\times A_{jl}(k, \omega') A_{lj}(k, \omega + \omega'). \end{aligned} \quad (10)$$

Here, $v^{jj}(k)$ is the diagonal element of the quasiparticle group velocity in the matrix form

$$\hat{v}(k) = \begin{pmatrix} \frac{\partial \hat{H}_k}{\partial k_x} & 0 \\ 0 & -\frac{\partial \hat{H}_k}{\partial k_x} \end{pmatrix}. \quad (11)$$

Figs. 4(a)-4(d) show the results for the optical conductivity calculated with the same scattering potentials as used to get Fig. 3(a)-3(d). With only spin domain-derived scattering [Fig. 4(a)], no Drude-like component appears at zero frequency in the optical conductivity, instead a finite frequency conductivity peak occurs around 0.3. This indicates that the system exhibits the "insulating" property.³² When only charge domain-derived scattering is considered [Fig. 4(b)], the Drude-like peak shows up and at the meantime the finite frequency peak remains. Optical conductivity involves the contribution from the quasiparticle excitations along the whole Fermi surface weighted by the quasiparticle group velocity. Due to the relative flat band structure near the antinodal region for the high- T_c cuprates, the zero frequency optical conductivity mainly comes from the quasiparticle excitations around the nodal region. In the case of only spin domain-derived scattering, the nodal region of the Fermi surface is gapped and therefore the quasiparticle spectral weight is suppressed around the nodal region as shown in Fig. 3(a), so that the zero-frequency Drude-like peak is absent and a finite frequency peak with its position being equal to the gap ($\approx 2V_s = 0.3$) occurs. For the charge domain-derived scattering, the gap opens around the hot spots and near the antinodal, but a large spectral weight situates around the nodal region, as can be seen from Fig. 3(b). Thus, the Drude-like peak emerges and the finite frequency peak remains (it is now situates at $\approx 2V_c = 0.34$). As shown in Fig. 3(c), with the increase of the charge domain-derived scattering V_c , the gap near the nodal region which is resulted from the spin domain-derived scattering will be suppressed gradually and correspondingly the spectral weight will be enhanced. As a result, the finite frequency peak in the optical conductivity is shifted to lower frequency and the zero frequency component is lifted up gradually [Fig. 4(c)].

When the charge domain-derived scattering is comparable to the spin one, the quasiparticles have noticeable spectra weight along the entire Fermi surface with its largest weight around the nodal region[Fig. 3(d)], then the Drude-like mode occurs at the zero frequency, and the finite frequency peak fades away and merges into the Drude-like peak, as shown in Fig. 4(d). The calculated results for the optical conductivity presented in Figs. 4(c) and 4(d) are consistent well with the experimental observations in the stripe state of $\text{La}_{1.275}\text{Nd}_{0.6}\text{Sr}_{0.125}\text{CuO}_4$ ¹⁵ and $\text{La}_{1.875}\text{Ba}_{0.125}\text{CuO}_4$ ¹⁸, respectively.

D. Discussion

We now discuss the implication of our theoretical results. As noted in the introduction, in $\text{La}_{1.275}\text{Nd}_{0.6}\text{Sr}_{0.125}\text{CuO}_4$ system, ARPES experiment has found that there is little or no low-energy spectral weight near the nodal region,³ and optical conductivity experiment has observed a finite frequency peak with almost the disappearance of the Drude mode, indicating an "insulating" stripe state.^{15,16} These spectroscopic features can be reproduced here with a strong spin domain-derived scattering potential $V_s = 0.15$ and a weak charge domain-derived potential $V_c = 0.08$ and $V_c = 0$, as shown in Figs. 3(a), 3(c), 4(a) and 4(c). Interestingly, in this parameter regime for the spin and charge domain-derived scattering, the SC order is destroyed as can be seen from Fig. 2(b). This is in consistent with the experimental fact that $\text{La}_{1.275}\text{Nd}_{0.6}\text{Sr}_{0.125}\text{CuO}_4$ is nonsuperconducting. In another cuprate $\text{La}_{1.875}\text{Ba}_{0.125}\text{CuO}_4$, ARPES spectra have identified the existence of high spectral intensity around the nodal region,¹³ and the optical conductivity measurement has observed a residual Drude peak without the finite frequency peak,¹⁸ pointing to a so-called nodal metal state.^{18,19,20,21,22,23} When comparable spin and charge domain-derived scattering potentials are assumed such as $V_s = 0.15$ and $V_c = 0.17$, we can reproduce these features consistently, as shown in Figs. 3(d) and 4(d). On the other hand, a weak superconductivity emerges in the otherwise nonsuperconducting regime (when only spin scattering potential V_{sc} is considered) with the increase of the charge domain-derived scattering potential[see Fig. 2(b)]. This suggests that the weak superconductivity in $\text{La}_{1.875}\text{Ba}_{0.125}\text{CuO}_4$ is likely beneficial from the metallic behaviors of the stripe state originated from a sufficient charge domain-derived scattering. The above mentioned consistent accounting for both divergent spectroscopic features observed in two families of high- T_c cuprates indicates that the stripe state may be intrinsically "insulating" or "metallic", depending on the relative strength of the spin and charge domain-derived scattering potentials. Specifically, a large spin domain-derived scattering potential favors the "in-

ulating" state, while a large charge domain-derived scattering potential the "metallic" state.

IV. CONCLUSION

We have calculated the SC order parameter, the spectral function and the optical conductivity in a stripe model with spin and charge domain-derived scattering potentials (V_s and V_c). The self-consistent calculation of the SC order parameter shows that the charge domain-derived scattering is less effective than the spin scattering on the suppression of superconductivity, and may even lead to the emergency of the SC order which is otherwise destroyed by the spin only scattering. For $V_s \gg V_c$, the zero-energy spectral weight disappears around the nodal points, and a finite energy peak appears in the optical conductivity with almost the disappearance of the Drude peak. But for $V_s \approx V_c$, the spectral weight concentrates on the nodal region, and a residual Drude peak exists in the optical conductivity without the finite energy peak. These results consistently account for the divergent spectroscopic properties observed experimentally in two families of high- T_c cuprates, and demonstrate that both the "insulating" and "metallic" behavior may be the intrinsic properties of the stripe state, depending on the relative strength of the spin and charge domain-derived scattering potentials.

V. ACKNOWLEDGEMENT

This project was supported by National Natural Science Foundation of China (Grant No. 10525415), the Ministry of Science and Technology of Science (Grants Nos. 2006CB601002, 2006CB921800), the China Postdoctoral Science Foundation (Grant No. 20080441039), and the Jiangsu Planned Projects for Postdoctoral Research Funds (Grant No. 0801008C).

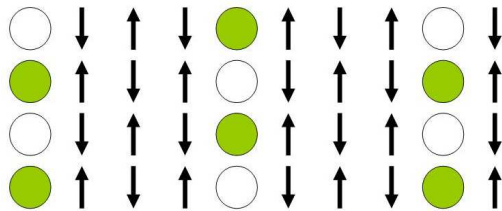


FIG. 1: (Color online) Schematic illustration of the charge and spin patterns in the 1/8 doped antiphase stripe state. Circles represent the charge domain wall (An empty circle indicates a hole density of one per site), and arrows the copper spins.

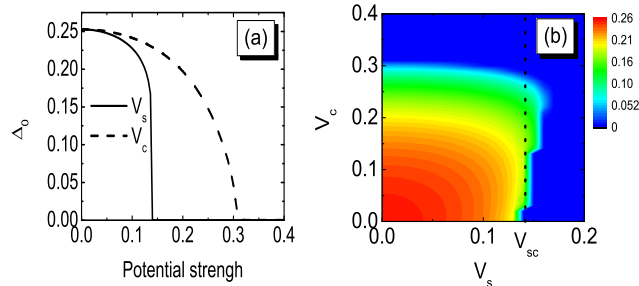


FIG. 2: (Color online) (a) Superconducting order parameter as a function of V_s and V_c , respectively. (b) A two-dimensional map of the superconducting order parameter in the parameter space of V_s and V_c .

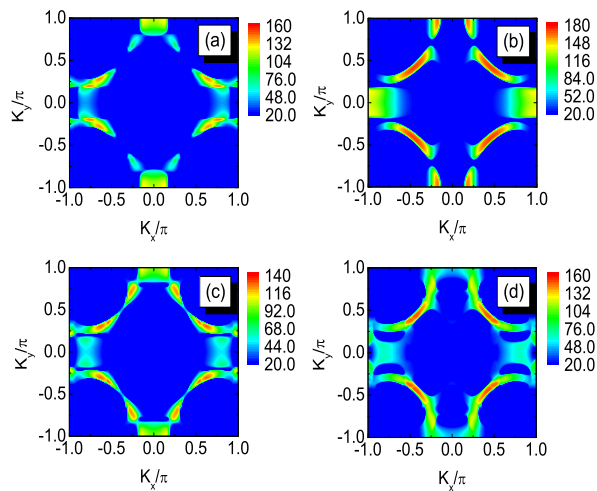


FIG. 3: (Color online) Spectral weight distribution for different spin (charge) domain-derived scattering potentials in the normal state with (a) $V_s = 0.15$ and $V_c = 0$, (b) $V_s = 0$ and $V_c = 0.17$, (c) $V_s = 0.15$ and $V_c = 0.08$, and (d) $V_s = 0.15$ and $V_c = 0.17$, respectively.

¹ S. A. Kivelson and I. P. Bindloss, E. Fradkin, V. Oganesyan, J. M. Tranquada, A. Kapitulnik, and C. Howald, *Rev. Mod. Phys.* **75**, 1201 (2003).
² J. M. Tranquada, B. J. Sternlieb, J. D. Axe, Y. Nakamura, and S. Uchida, *Nature* **375**, 561 (1995).
³ X. J. Zhou, P. Bogdanov, S. A. Kellar, T. Noda, H. Eisaki, S. Uchida, Z. Hussain, and Z.-X. Shen, *Science* **286**, 268 (1999).
⁴ J. M. Tranquada, H. Woo, T. G. Perring, H. Goka, G. D. Gu, G. Xu, M. Fujita, and K. Yamada, *Nature* **429** 534

(2004).

⁵ P. Abbamonte, A. Rusydi, S. Smadici, G. D. Gu, G. A. Sawatzky and D. L. Feng, *Nat. Phys.* **1** 155 (2005).
⁶ S-W. Cheong, G. Aeppli, T. E. Mason, H. Mook, S. M. Hayden, P. C. Canfield, Z. Fisk, K. N. Clausen, and J. L. Martinez, *Phys. Rev. Lett.* **67**, 1791 (1991).
⁷ T. E. Mason, G. Aeppli, and H. A. Mook, *Phys. Rev. Lett.* **68**, 1414 (1992).
⁸ A. Bianconi, N. L. Saini, A. Lanzara, M. Missori, T. Rossetti, H. Oyanagi, H. Yamaguchi, K. Oka, and T. Ito, *Phys.*

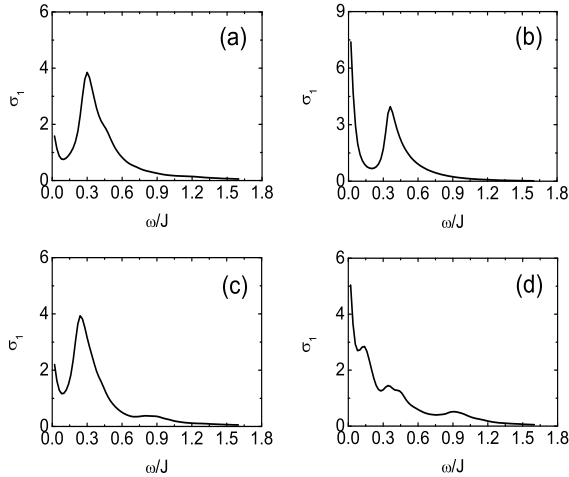


FIG. 4: In-plane optical conductivity as a function of frequency for different spin (charge) domain-derived scattering potentials in the $1/8$ antiphase stripe with the SC order parameter $\Delta = 0$. (a) $V_s = 0.15$ and $V_c = 0$, (b) $V_s = 0$ and $V_c = 0.17$, (c) $V_s = 0.15$ and $V_c = 0.08$, and (d) $V_s = 0.15$ and $V_c = 0.17$.

- Rev. Lett. **76**, 3412 (1996).
- ⁹ K. Yamada, C. H. Lee, K. Kurahashi, J. Wada, S. Wakimoto, S. Ueki, H. Kimura, Y. Endoh, S. Hosoya, G. Shirane, R. J. Birgeneau, M. Greven, M. A. Kastner, and Y. J. Kim, Phys. Rev. B **57**, 6165 (1998).
 - ¹⁰ B. O. Wells, Y. S. Lee, M. A. Kastner, R. J. Christianson, R. J. Birgeneau, K. Yamada, Y. Endoh, and G. Shirane, Science **277**, 1067 (1997).
 - ¹¹ Y. S. Lee, R. J. Birgeneau, M. A. Kastner, Y. Endoh, S. Wakimoto, K. Yamada, R. W. Erwin, S.-H. Lee, and G. Shirane, Phys. Rev. B **60**, 3643 (1999).
 - ¹² H. A. Mook, P. Dai, S. M. Hayden, G. Aeppli, T. G. Perring, and F. Doğan, Nature **395**, 580 (1998).
 - ¹³ T. Valla, A. V. Fedorov, J. Lee, J. C. Davis, and G. D. Gu, Science **314**, 1914 (2006).
 - ¹⁴ X. J. Zhou, T. Yoshida, S. A. Kellar, P. V. Bogdanov, E. D. Lu, A. Lanzara, M. Nakamura, T. Noda, T. Kakeshita, H. Eisaki, S. Uchida, A. Fujimori, Z. Hussain, and Z.-X. Shen, Phys. Rev. Lett. **86**, 5578 (2001).
 - ¹⁵ M. Dumm, and D. N. Basov, Seiki Komiya, Yasushi Abe, and Yoichi Ando, Phys. Rev. Lett. **88**, 147003 (2002).
 - ¹⁶ M. Ortolani, P. Calvani, S. Lupi, U. Schade, A. Perla, M. Fujita, and K. Yamada, Phys. Rev. B **73**, 184508 (2006).
 - ¹⁷ C. Castellani, C. Di Castro, M. Grilli, A. Perali, Physica C **341-348**, 1739 (2000).
 - ¹⁸ C. C. Homes, S. V. Dordevic, G. D. Gu, Q. Li, T. Valla, and J. M. Tranquada, Phys. Rev. Lett. **96**, 257002 (2006).
 - ¹⁹ Y. Ando, A. N. Lavrov, S. Komiya, K. Segawa, and X. F. Sun, Phys. Rev. Lett. **87**, 017001 (2001).
 - ²⁰ X. J. Zhou, T. Yoshida, A. Lanzara, P. V. Bogdanov, S. A. Kellar, K. M. Shen, W. L. Yang, F. Ronning, T. Sasagawa, T. Kakeshita, T. Noda, H. Eisaki, S. Uchida, C. T. Lin, F. Zhou, J. W. Xiong, W. X. Ti, Z. X. Zhao, A. Fujimori, Z. Hussain, and Z.-X. Shen, Nature (London) **423**, 398 (2003).
 - ²¹ M. Dumm, S. Komiya, Y. Ando, and D. N. Basov, Phys. Rev. Lett. **91**, 077004 (2003).
 - ²² M. Sutherland, D. G. Hawthorn, R. W. Hill, F. Ronning, S. Wakimoto, H. Zhang, C. Proust, E. Boaknin, C. Lupien, L. Taillefer, R. Liang, D. A. Bonn, W. N. Hardy, R. Gagnon, N. E. Hussey, T. Kimura, M. Nohara, and H. Takagi, Phys. Rev. B **67**, 174520 (2003).
 - ²³ Y. S. Lee, K. Segawa, Y. Ando, and D. N. Basov, Phys. Rev. B **70**, 014518 (2004).
 - ²⁴ T. Tohyama, S. Nagai, Y. Shibata, and S. Maekawa, Phys. Rev. Rev. **82**, 4910 (1999).
 - ²⁵ R. S. Markiewicz, Phys. Rev. B **62**, 1252 (2000).
 - ²⁶ I. Martin, G. Ortiz, A. V. Balatsky, and A. R. Bishop, Europhys. Lett. **56**, 849 (2001).
 - ²⁷ J. Lorenzana, and G. Seibold, Phys. Rev. Rev. **90**, 066404 (2003).
 - ²⁸ A. J. Millis, and M. R. Norman, Phys. Rev. B **76**, 220503(R) (2007).
 - ²⁹ P. A. Lee, N. Nagaosa, and X. G. Wen, Rev. Mod. Phys. **78**, 17 (2006).
 - ³⁰ J. X. Li, C. Y. Mou, and T. K. Lee, Phys. Rev. B **62**, 640 (2000).
 - ³¹ E. Berg, E. Fradkin, E.-A. Kim, S. A. Kivelson, V. Oganesyan, J. M. Tranquada, and S. C. Zhang, Phys. Rev. Lett. **99**, 127003 (2007).
 - ³² The term "insulating" state used here follows Refs. 14,16, 18 to indicate a strong suppression of Drude peak in the optical conductivity. In fact, the spectral weight at the Fermi level will not be fully gapped out, so it is not a true insulating state. We use the term here is to facilitate our comparison with the experiments[Refs. 14,16,18].